Experimental Reconstruction of the Few-Photon Nonlinear Scattering Matrix from a Single Quantum Dot in a Nanophotonic Waveguide

Hanna Le Jeannic,[1,*] Tomás Ramos,[2,3,†] Signe F. Simonsen,[1] Tommaso Pregnolato,[1] Zhe Liu,[1] Rüdiger Schott,[4] Andreas D. Wieck,[4] Arne Ludwig,[4] Nir Rotenberg,[1] Juan José García-Ripoll,[2] and Peter Lodahl[1,‡]

[1]*Center for Hybrid Quantum Networks (Hy-Q), Niels Bohr Institute, University of Copenhagen, Blegdamsvej 17, DK-2100 Copenhagen, Denmark*

[2]*Instituto de Física Fundamental IFF-CSIC, Calle Serrano 113b, Madrid 28006, Spain*

[3]*DAiTALab, Facultad de Estudios Interdisciplinarios, Universidad Mayor, Santiago, Chile*

[4]*Lehrstuhl für Angewandte Festkörperphysik, Ruhr-Universität, Universitätsstrasse 150, D-44780 Bochum, Germany*

(Received 30 May 2020; accepted 16 December 2020; published 13 January 2021)

Coherent photon-emitter interfaces offer a way to mediate efficient nonlinear photon-photon interactions, much needed for quantum information processing. Here we experimentally study the case of a two-level emitter, a quantum dot, coupled to a single optical mode in a nanophotonic waveguide. We carry out few-photon transport experiments and record the statistics of the light to reconstruct the scattering matrix elements of one- and two-photon components. This provides direct insight to the complex nonlinear photon interaction that contains rich many-body physics.

DOI: 10.1103/PhysRevLett.126.023603

An efficient and reliable photon-photon nonlinearity is a key building block for photonic quantum information processing. One approach exploits postselection after photon interference, but is resource demanding in requiring many auxiliary photons [1]. An alternative and potentially more appealing strategy is to exploit an efficiently interfaced quantum emitter to introduce a direct photon-photon interaction [2,3]. This approach requires highly efficient and coherent light-matter interaction in order to be sensitive to single quanta of light. It has been a long lasting challenge in quantum optics, and various strategies have been pursued using, e.g., Rydberg blockade interaction in atomic ensembles [4,5] and single emitters in high finesse optical cavities [6,7], as well as superconducting stripline resonators [8–10]. Recently, significant progress has been achieved in photonic waveguides, including hollow fibers [11] or nanofibers coupled to atomics ensembles [12], or with single atoms [13] and single solid-state emitters [14–18]. In particular, solid-state quantum dots (QDs) in nanophotonics structures constitute a mature platform where scalable coherent single-photon sources [19,20] have been developed, at the core of the implementation of quantum information processing [21].

QDs coupled to photonic-crystal waveguides provide a sophisticated platform to study few-photon interactions and quantum nonlinear optics [2,22]. These devices can exhibit near-unity light-matter coupling efficiency ($\beta \geq 0.98$ [23]) and nonlinear interaction sensitive at the level of single photons [14,16]. Moreover, near-transform-limited emission lines have been demonstrated with QDs [24] and recently also in photonic-crystal waveguides [25]. The combination of unity coupling efficiency and low dephasing enables the deterministic scattering of few photons by a QD operating as a two-level emitter (TLE). The study of such scattering problems is a blooming area in quantum nonlinear optics [26,27]. For the theoretical description, a range of new methods have been developed using the Bethe ansatz [28,29], input-output theory [30–33], Lippmann-Schwinger formalism [34–36], wave function ansatz [37], diagrammatic methods [38,39], path integrals [40], and polaron ansatz [41,42]. Deterministic photon scattering processes have important applications for the realization of efficient photon sorting and deterministic Bell-state analyzers [43,44] and can induce intricate many-body phenomena, including strong photon correlations and complex photon bound states [28,29,45,46]. Despite this extensive theoretical work, it remains an open problem to isolate and characterize photon-photon interactions in the laboratory and to develop and implement few- or multi-photon tomographic reconstruction techniques [47] beyond the single-photon regime.

This Letter presents the experimental reconstruction of the few-photon scattering processes of a QD in a photonic-crystal waveguide. While the coherent scattering of single photons from a TLE is simple—the photons are either elastically reflected or transmitted [cf. Fig. 1(a) and Ref. [48]]—the two-photon scattering processes are much more complex. In this case, different combinations of photon reflections and transmissions are possible, as shown in Fig. 1(b). Furthermore, the scattered photons become highly correlated from the interaction with the TLE [29]. We unravel these scattering processes by recording the photon statistics of the transmission and reflection outputs of a QD-waveguide system in the continuous wave (cw)

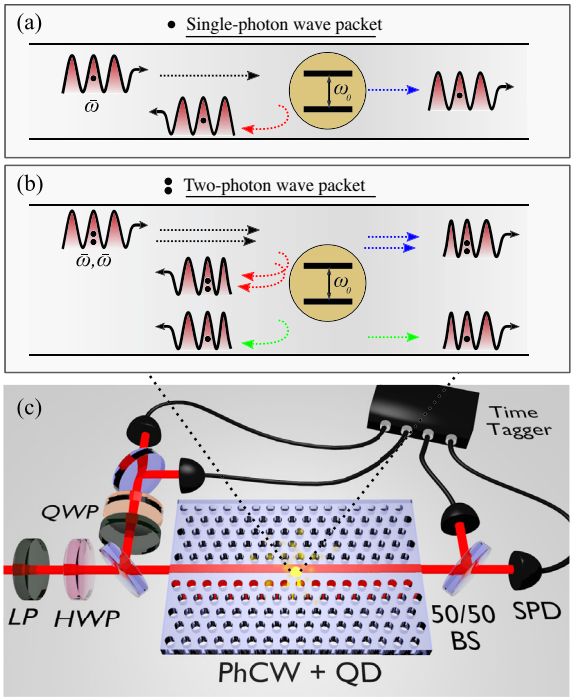

FIG. 1. (a),(b) Illustration of single- and two-photon scattering processes for a TLE in a waveguide. In the former case, either elastic reflection or transmission may occur. In the latter case, the two photons may exchange energy via the interaction with the TLE, leading to different scattering processes. (c) Experimental setup to extract the few-photon scattering matrices of the system from intensity I_t and photon-correlation measurements $g^{(2)}_{tt}$, $g^{(2)}_{rr}$, and $g^{(2)}_{tr}$ between different scattering channels. The QD is embedded in a photonic-crystal waveguide (PhCW) and excited by a cw laser source. Beam splitters (BS), single-photon detectors (SPDs), and an electronic time tagger are used to record second-order photon correlations. Polarizing optical elements, such as two linear polarizers (LPs), a half- and a quarter-wave plate (HWP and QWP, respectively) are used for extinction of the laser light and collection of the reflected light from the QD.

regime [cf. Fig. 1(c)]. Even in cw operation, photon-photon interactions can be extracted from photon-correlation measurements, despite the low probability that incoming photons overlap in time. Our method extends a previous theoretical proposal of reconstructing multiphoton scattering properties [47], where the extension to photocorrelation measurements makes it insensitive to any off-chip coupling and detection inefficiencies.

Consider first for simplicity the case of a coherent TLE without dephasing that is symmetrically coupled to a waveguide (i.e., no chiral coupling [49,50]). Here, an incoming single-photon wave packet may scatter from this system producing an output state

$$|\Psi^{(1)}_{\mathrm{out}}\rangle = \sum_{\mu=t,r}\int d\omega f_{\bar{\omega}}(\omega)\chi^{\mu}(\omega)|1^{\mu}_{\omega}\rangle \tag{1}$$

that is a superposition of single-photon Fock states $|1^{\mu}_{\omega}>$ of frequency ω, which are either transmitted ($\mu = t$) or reflected ($\mu = r$) [cf. Fig. 1(a)]. Both contributions are weighted by the incoming wave packet profile $f_{\bar{\omega}}(\omega)$, centered around frequency $\bar{\omega}$, and by the single-photon transmission [$\chi^t(\omega) \coloneqq t(\omega)$] and reflection [$\chi^r(\omega) \coloneqq r(\omega)$] scattering coefficients, given by

$$t(\omega) = 1 + r(\omega), \qquad r(\omega) = \frac{-\beta\gamma_{\mathrm{tot}}}{\gamma_{\mathrm{tot}} - 2i(\omega-\omega_0)}. \tag{2}$$

Here, $\omega - \omega_0$ is the TLE-photon detuning, $\beta = \gamma_{\mathrm{wg}}/\gamma_{\mathrm{tot}}$ is the waveguide coupling efficiency, and $\gamma_{\mathrm{tot}} = \gamma_{\mathrm{wg}} + \gamma_l$ is the total TLE decay rate, which includes the TLE-waveguide coupling rate γ_{wg} and the loss into unguided modes γ_l. As pointed out in Ref. [32], the complex coefficients χ^{μ}_{ω} fully characterize the single-photon scattering and satisfy $t(\omega) = 1 + r(\omega)$ even in the presence of loss or dephasing. In contrast, the intensity at transmission $I_t \geq 0$ and reflection $I_r \geq 0$ quantify the output flux and satisfy $I_t + I_r \leq 1$, where the equality only holds in the absence of decoherence channels.

Nonlinear quantum optical effects arise when an i ncoming two-photon wave packet scatters off the TLE. Here, two incoming photons with frequencies ω_1, ω_2 may exchange energy via the TLE and thereby become correlated outgoing photons with frequencies ν_1, ν_2. This process can happen either when both photons are transmitted, both reflected, or one transmitted and one reflected [cf. Fig. 1(b)], and thus the output state $|\Psi^{(2)}_{\mathrm{out}}\rangle$ is a superposition of all these possibilities, i.e., [30],

$$\begin{aligned}|\Psi^{(2)}_{\mathrm{out}}\rangle = \sum_{\mu,\mu'=t,r}\iint d\omega_1 d\omega_2 \frac{1}{\sqrt{2}} f_{\bar{\omega}}(\omega_1) f_{\bar{\omega}}(\omega_2) \\ \times \iint d\nu_1 d\nu_2 \{\chi^{\mu}(\omega_1)\chi^{\mu'}(\omega_2)\delta(\nu_2-\omega_2)\delta(\nu_1-\omega_1) \\ + \frac{1}{2} T_{\nu_1\nu_2\omega_1\omega_2}\delta(\nu_1+\nu_2-\omega_1-\omega_2)\}|1^{\mu}_{\nu_1}\rangle|1^{\mu'}_{\nu_2}\rangle.\end{aligned} \tag{3}$$

The first term $\sim\chi^{\mu}(\omega_1)\chi^{\mu'}(\omega_2)$ in Eq. (3) corresponds to independent single-photon scattering events, and thus each photon conserves its own energy ($\nu_1 = \omega_1, \nu_2 = \omega_2$). In the last term, however, the correlated scattering coefficient $T_{\nu_1\nu_2\omega_1\omega_2}$ describes two photons acquiring a nonlinear phase shift and exchanging energy so that only the total energy is conserved ($\nu_1 + \nu_2 = \omega_1 + \omega_2$). For a TLE in a conventional waveguide [30],

$$T_{\nu_1\nu_2\omega_2\omega_1} = \frac{4}{\pi\beta\gamma_{\mathrm{tot}}}\frac{r(\nu_1)r(\nu_2)r(\omega_1)r_(\omega_2)}{r(\frac{\omega_1+\omega_2}{2})}. \tag{4}$$

This scattering matrix fully characterizes two-photon interactions, including the spectral entanglement and photon-bound states induced by the TLE [28,29]. The main

objective in this Letter is to extract this information from experimental data, as described below. The analysis is generalized in the Supplemental Material [51] to include experimental imperfections, including pure dephasing of the QD transition and weak Fano resonance effects.

We now describe the reconstruction protocol to experimentally characterize the nonlinear few-photon scattering processes. We follow the main idea of Ref. [47], which consists of illuminating the TLE with an attenuated coherent state ($|\alpha|^2 \ll 1$) through one input of the waveguide. Light scatters from the TLE, creating a superposition of vacuum $|0\rangle$ and scattering output states for one $|\Psi^{(1)}_{\mathrm{out}}\rangle$, two $|\Psi^{(2)}_{\mathrm{out}}\rangle$ [cf. Eqs. (1) and (3)], or more photons

$$|\Psi^{(\alpha)}_{\mathrm{out}}\rangle = |0\rangle + \alpha|\Psi^{(1)}_{\mathrm{out}}\rangle + \frac{\alpha^2}{\sqrt{2}}|\Psi^{(2)}_{\mathrm{out}}\rangle + \mathcal{O}(\alpha^3). \quad (5)$$

The two-photon processes can be recorded in second-order correlation measurements $g^{(2)}_{\mu\mu'}$ between different output directions μ, μ' [cf. Fig. 1(c)]. For a monochromatic cw laser input of frequency ω, we find that [51,55]

$$g^{(2)}_{\mu\mu'}(\tau) = \frac{|\chi^{\mu}(\omega)\chi^{\mu'}(\omega) + \mathcal{T}(\omega,\tau)|^2}{|\chi^{\mu}(\omega)\chi^{\mu'}(\omega)|^2} + \mathcal{O}(|\alpha|^2). \quad (6)$$

Here, τ is the time delay between the two photon detections, and $\mathcal{T}(\omega,\tau)$ is the Fourier transformed two-photon scattering coefficient defined as

$$\mathcal{T}(\omega,\tau) = \frac{1}{2}\int d\Delta e^{-i\Delta\tau} T_{\omega-\Delta,\omega+\Delta,\omega,\omega}. \quad (7)$$

The isotropy of the photon-photon interaction, i.e., the absence of a preferred direction of emission among left and right, allows us to reconstruct experimentally the real part of this Fourier transform as [51,55]

$$\mathrm{Re}[\mathcal{T}(\omega,\tau)] = g^{(2)}_{tt}\frac{|t(\omega)|^4}{2} + g^{(2)}_{rr}\frac{|r(\omega)|^4}{2} - g^{(2)}_{tr}|t(\omega)r(\omega)|^2. \quad (8)$$

We note that the protocol requires correlation measurements in all directions $g^{(2)}_{tt}$, $g^{(2)}_{rr}$, and $g^{(2)}_{tr}$, as well as the single-photon coefficients $t(\omega)$ and $r(\omega)$. From the real part of $\mathcal{T}$ we infer the imaginary part using the Kramers-Kronig (KK) relation, $\mathrm{Im}[\mathcal{T}(\omega,\tau)] = (1/\pi)\mathcal{P}\int d\omega' \{\mathrm{Re}[\mathcal{T}(\omega',\tau)]/(\omega-\omega')\}$ [51]. Finally, an inverse Fourier transform, $T_{\omega-\Delta,\omega+\Delta,\omega,\omega} = (1/\pi)\int d\tau e^{i\Delta\tau}\mathcal{T}(\omega,\tau)$, provides the two-photon scattering matrix.

Remarkably, a measurement of the transmitted intensity $I_t(\omega) \geq 0$ suffices to extract the amplitude and phase of both complex single-photon scattering coefficients $t(\omega)$ and $r(\omega)$ [32]. Specifically, for a weak monochromatic coherent input

$$I_t(\omega) = \beta - 1 + (2-\beta)\mathrm{Re}[t(\omega)] + \mathcal{O}(|\alpha|^2). \quad (9)$$

From this we can infer the real part of $t(\omega)$, even in the presence of correlated dephasing noise [32]. Using a KK relation (cf. Supplemental Material [51] for details), we then compute the imaginary part, obtaining both $t(\omega)$ and $r(\omega) = t(\omega) - 1$.

We now turn to the experimental demonstration of the few-photon scattering reconstruction. We apply it to a self-assembled InGaAs QD embedded in a suspended photonic-crystal waveguide. A *p-i-n* diode heterostructure enables electrical contacting of the sample in order to stabilize the charge environment and tune the QD. Further details of the sample wafer can be found in Ref. [56]. The sample is kept at $T = 1.6$ K and a weak tunable cw laser at 938 nm (linewidth ≤ 10 kHz, locked within a precision of 50 MHz) is launched through the waveguide via high-efficiency grating couplers [51,57]. Finally, the output photons are sent to superconducting nanowire single-photon detectors, with quantum efficiency ≥ 0.9 and time jitter below 100 ps, to record the frequency-dependent intensity and second-order photon-correlation functions.

Figure 2(a) shows the transmitted intensity $I_t(\omega)$ when scanning through the QD resonance for weak excitation (on average less than 0.1 photons per QD lifetime). The extinction of transmission on resonance exceeds 85%, a direct testimony of the efficiency and coherence of the photon-emitter interaction. The non-Lorentzian and

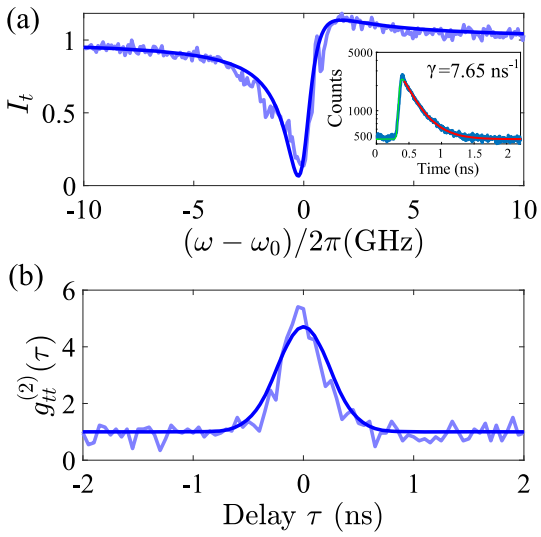

FIG. 2. (a) Measured (light blue) and fitted (dark blue) transmission intensity $I_t(\omega)$ as a function of the detuning of the excitation laser from the QD resonance. Inset: time resolved dynamics of the QD (in logarithmic scale) and exponentially decaying fitting function, convolved with the instrument response of the detector, to characterize the radiative decay rate. (b) Measured (light blue) and fitted (dark blue) second-order correlation function $g^{(2)}_{tt}(\tau)$ in transmission, with time delay τ, obtained on resonance ($\omega \approx \omega_0$).

asymmetric line shape, originates from Fano resonance effects due to weak reflections at the ends of the waveguide [14,17]. Such reflections induce a very low finesse cavity that, depending on the overall intensity normalization (more details in Supplemental Material [51]), can give I_t values higher than 1. We record a transition linewidth of ≈1.6 GHz. For comparison, the spontaneous emission decay rate is measured to be $\gamma_{\mathrm{tot}} = \gamma_{\mathrm{wg}} + \gamma_l = 7.65 \pm 0.08\ \mathrm{ns}^{-1}$ [cf. inset of Fig. 2(a)], corresponding to a transform-limited linewidth of 1.22 GHz, meaning that additional broadenings due to phonons and slow spectral diffusion are less important. A full study of the statistics of QD linewidths in photonic-crystal waveguides is published elsewhere [25].

Figure 2(b) shows the second-order correlation function $g^{(2)}_{tt}(\tau)$ measured in transmission and for the same excitation conditions. It displays a pronounced bunching of $g^{(2)}_{tt}(0) \simeq 5$, which is significantly higher than in previously reported QD-waveguide experiments [14,16,17] due to the substantial decoherence reduction achieved in our photon-emitter interface. The large bunching demonstrates that the incoming Poissonian photon distribution is significantly altered by the interaction with the QD and is the experimental signature of the correlated photon-photon interaction studied in the present Letter.

In order to implement the two-photon reconstruction protocol, the essential governing parameters of the system must be determined first. To do so, we additionally measure the transmission intensities $I_t(\omega)$ at various excitation powers, as well as photon correlations in all directions $g^{(2)}_{tt}$, $g^{(2)}_{rr}$, and $g^{(2)}_{tr}$. By modeling this entire dataset using a least squares fit, we arrive at a descriptive parameter set of $\beta = 0.87[0.83, 0.91]$ and dephasing rate $\gamma_d \simeq 0[0, 0.02]\gamma_{\mathrm{tot}}$, consistent with results from the literature [17,23]. In the analysis, we also include the finite detector response time, residual spectral diffusion of the QD, background emission stemming from imperfect laser extinction or blinking of the QD state, and minor Fano resonance effects. We define the error ranges presented above as the 95% confidence interval of each fitted parameter (more details in Supplemental Material [51]).

As a first step, we use Eq. (9) and the KK relation (adapted for experimental imperfections, see Supplemental Material [51]) to extract the single-photon transmission and reflection coefficients from the intensity data $I_t(\omega)$. We plot the experimental amplitude and phase of both $t(\omega)$ and $r(\omega)$ in Fig. 3 and observe excellent agreement with theory for the experimentally determined parameters. The asymmetry of the resonances, a minor frequency shift, and the nonzero phase shift away from the resonance are again here due to the Fano effect, cf. Supplemental Material for details [51]. We record an experimental maximal single-photon phase shift of ≈150° in reflection and ≈ − 40° in transmission.

We can now extract the real part of the intrinsic two-photon scattering coefficient $\mathcal{T}(\omega, \tau)$ based on Eq. (8),

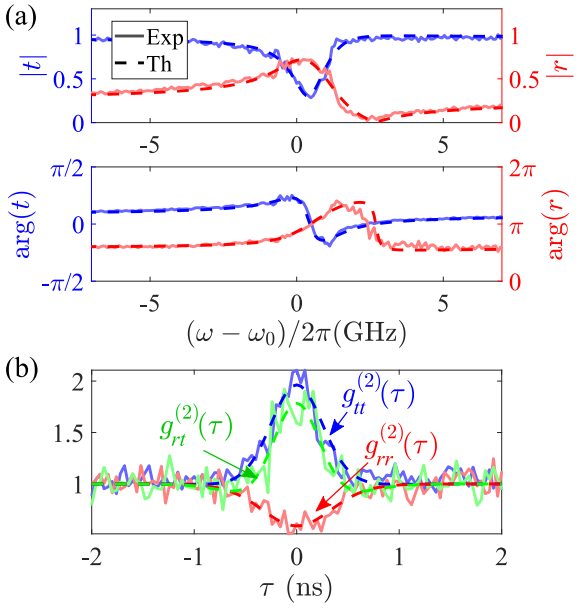

FIG. 3. (a) Experimentally reconstructed (solid line) modulus and phase of the complex single-photon transmission (blue) and reflection (red) coefficients and comparison to theory (dashed line). (b) Experimentally acquired second-order correlation functions for the three different configurations: $g^{(2)}_{tt}$ (blue), $g^{(2)}_{rr}$ (red), and $g^{(2)}_{rt}$ (green). The measurements are well fitted by the theoretical model including imperfections (dashed lines).

$\chi^{\mu}(\omega)$, and the photo-correlation measurements in all directions $g^{(2)}_{\mu\mu'}(\tau)$. Special care was taken to suppress residual stray scattering from the excitation laser for the measurements in reflection to improve the signal-to-noise ratio. The excitation power was a factor of ≈3 higher than in Fig. 2(b). The data are plotted in Fig. 3(b), displaying bunching in $g^{(2)}_{tt}$ and $g^{(2)}_{rt}$, and antibunching in $g^{(2)}_{rr}$. We find excellent agreement between experiment and theory using the system parameters and the modeling of imperfections discussed above, cf. Supplemental Material [51] for details.

The experimental reconstruction of the real part of the intrinsic two-photon correlations $\mathcal{T}$, obtained by processing the experimental data, is shown in Fig. 4(a). The reconstructed line shape and depth is found to be in accordance with the theoretical prediction for a TLE, $\mathcal{T}(\omega, \tau) = -r(\omega)^2 e^{-|\tau|(\gamma_{\mathrm{tot}}/2 - i[\omega - \omega_0])}$, when including all the discussed imperfections [see black line in Fig. 4(a)]. This is, to our knowledge, the first experimental reconstruction of the two-photon nonlinear response. This analysis pinpoints the genuine strength of correlated two-photon response of the QD-waveguide system and can be extended further to extract the full matrix in Eq. (4) straightforwardly by scanning the input laser frequency ω and applying the KK relation [51]. This requires high-frequency resolution and a broad scanning interval $\sim 5\gamma_{\mathrm{tot}}$ to accurately determine the amplitude and phase [58].

The signal-to-noise ratio in Fig. 4(a) is limited by the photon collection efficiency, especially in reflection.

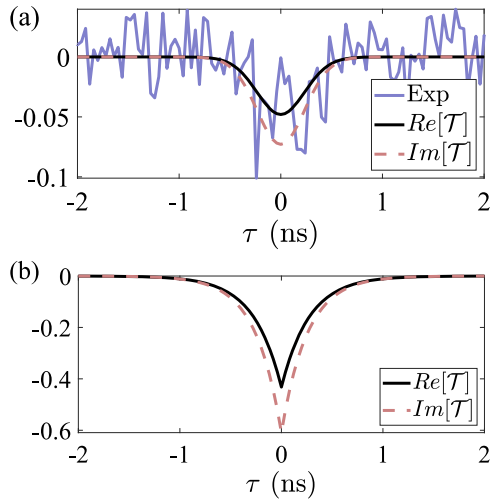

FIG. 4. (a) Real part of the two-photon correlated coefficient $\mathrm{Re}[\mathcal{T}]$ reconstructed from experimental data (blue) and comparison to theory (black). The theoretical imaginary part $\mathrm{Im}[\mathcal{T}]$ is also included (dashed pink). (b) Theoretical prediction of the real (solid black) and imaginary (dashed pink) parts of $\mathcal{T}$ in the absence of external experimental imperfections.

Nevertheless, this can be substantially improved by designing a waveguide with three different coupling gratings, so that the excitation and reflected signals are spatially separated (cf. Sec. I. F. of Supplemental Material [51]). Another important experimental challenge is to further improve the electrical noise performance of the device so that spectral diffusion of the QD can be strongly suppressed. Progress on this direction has been very recently obtained [25]. Alternatively, a feedback loop could be implemented to adjust for the slow frequency drift [59]. When fully correcting for these effects, we predict an order of magnitude enhancement of the two-photon nonlinearity induced by the QD [cf. Fig. 4(b)], which would lead to a higher signal-to-noise ratio in the reconstruction. Moreover, we also predict an enhancement by 2 orders of magnitude in the bunching of $g_{tt}^{(2)}$ and $g_{tr}^{(2)}$ (see Fig. S2 of Supplemental Material [51]), which shows the capabilities of the highly coherent light-matter interface.

In summary, we have presented measurements of the one- and two-photon components of the scattering matrix of a single QD in a photonic-crystal waveguide excited by a weak laser source. The applied method relies on intensity and second-order photon-correlation measurements, making it well suited for current experimental settings and devices. Specifically, we have presented the first experimental reconstruction of the intrinsic two-photon scattering correlations that are induced by the appearance of the two-photon bound state [28,29]. Extending this approach to three- or even N-photon scattering processes requires measuring N-order photon correlations in all 2^N possibilities of propagation direction, but this will be discussed elsewhere [55].

This type of reconstruction technique will enable further developments within quantum nonlinear optics, where a thorough understanding of the nonlinear response is required in potential applications of the nanophotonic hardware. For instance, it has been shown that the two-photon scattering processes, if properly controlled via the incoming photon pulse lengths, can be the basis of deterministic photon sorting, which enables the construction of deterministic Bell analyzers and photonic gates [43,44]. Furthermore, the presence of exotic photon bound states provides a route to study complex many-body quantum physics [29,46].

The authors would like to thank A. S. Sørensen for fruitful discussions. We gratefully acknowledge financial support from Danmarks Grundforskningsfond (DNRF 139, Hy-Q Center for Hybrid Quantum Networks), H2020 European Research Council (ERC) (SCALE), Styrelsen for Forskning og Innovation (FI) (5072-00016B QUANTECH), Bundesministerium fur Bildung und Forschung (BMBF) (16KIS0867, Q.Link.X), and Deutsche Forschungsgemeinschaft (DFG) (TRR 160). T. R. and J. J. G.-R. acknowledge support from Project No. PGC2018-094792-B-I00 (MCIU/AEI/FEDER, UE), CAM/FEDER Project No. S2018/TCS-4342 (QUITEMAD-CM), and CSIC Quantum Technology Platform PT-001. T. R. further acknowledges funding from the EU Horizon 2020 program under the Marie Skłodowska-Curie Grant Agreement No. 798397.

*hanna.lejeannic@nbi.ku.dk
†t.ramos.delrio@gmail.com
‡lodahl@nbi.ku.dk

[1] T. D. Ladd, F. Jelezko, R. Laflamme, Y. Nakamura, C. Monroe, and J. L. O'Brien, Nature (London) **464**, 45 (2010).
[2] D. E. Chang, V. Vuletić, and M. D. Lukin, Nat. Photonics **8**, 685 (2014).
[3] P. Lodahl, S. Mahmoodian, and S. Stobbe, Rev. Mod. Phys. **87**, 347 (2015).
[4] D. Tiarks, S. Schmidt-Eberle, T. Stolz, G. Rempe, and S. Dürr, Nat. Phys. **15**, 124 (2018).
[5] S. Baur, D. Tiarks, G. Rempe, and S. Dürr, Phys. Rev. Lett. **112**, 073901 (2014).
[6] A. Reiserer, N. Kalb, G. Rempe, and S. Ritter, Nature (London) **508**, 237 (2014).
[7] D. Najer, I. Söllner, P. Sekatski, V. Dolique, M. C. Löbl, D. Riedel, R. Schott, S. Starosielec, S. R. Valentin, A. D. Wieck, N. Sangouard, A. Ludwig, and R. J. Warburton, Nature (London) **575**, 622 (2019).
[8] F. Deppe, M. Mariantoni, E. P. Menzel, A. Marx, S. Saito, K. Kakuyanagi, H. Tanaka, T. Meno, K. Semba, H. Takayanagi *et al.*, Nat. Phys. **4**, 686 (2008).
[9] M. Mirhosseini, E. Kim, X. Zhang, A. Sipahigil, P. B. Dieterle, A. J. Keeler, A. Asenjo-Garcia, D. E. Chang, and O. Painter, Nature (London) **569**, 692 (2019).

[10] C. Lang, D. Bozyigit, C. Eichler, L. Steffen, J. M. Fink, A. A. Abdumalikov, M. Baur, S. Filipp, M. P. da Silva, A. Blais, and A. Wallraff, Phys. Rev. Lett. **106**, 243601 (2011).

[11] M. Bajcsy, S. Hofferberth, V. Balic, T. Peyronel, M. Hafezi, A. S. Zibrov, V. Vuletić, and M. D. Lukin, Phys. Rev. Lett. **102**, 203902 (2009).

[12] A. S. Prasad, J. Hinney, S. Mahmoodian, K. Hammerer, S. Rind, P. Schneeweiss, A. S. Sørensen, J. Volz, and A. Rauschenbeutel, arXiv:1911.09701.

[13] A. Goban, C.-L. Hung, S.-P. Yu, J. Hood, J. Muniz, J. Lee, M. Martin, A. McClung, K. Choi, D. Chang, O. Painter, and H. J. Kimble, Nat. Commun. **5**, 3808 (2014).

[14] A. Javadi, I. Söllner, M. Arcari, S. L. Hansen, L. Midolo, S. Mahmoodian, G. Kiršanskė, T. Pregnolato, E. H. Lee, J. D. Song *et al.*, Nat. Commun. **6**, 8655 (2015).

[15] H. Thyrrestrup, G. Kiršanskė, H. Le Jeannic, T. Pregnolato, L. Zhai, L. Raahauge, L. Midolo, N. Rotenberg, A. Javadi, R. Schott, A. D. Wieck, A. Ludwig, M. C. Löbl, I. Söllner, R. J. Warburton, and P. Lodahl, Nano Lett. **18**, 1801 (2018).

[16] D. Hallett, A. P. Foster, D. L. Hurst, B. Royall, P. Kok, E. Clarke, I. E. Itskevich, A. M. Fox, M. S. Skolnick, and L. R. Wilson, Optica **5**, 644 (2018).

[17] A. P. Foster, D. Hallett, I. V. Iorsh, S. J. Sheldon, M. R. Godsland, B. Royall, E. Clarke, I. A. Shelykh, A. M. Fox, M. S. Skolnick, I. E. Itskevich, and L. R. Wilson, Phys. Rev. Lett. **122**, 173603 (2019).

[18] A. Sipahigil, R. E. Evans, D. D. Sukachev, M. J. Burek, J. Borregaard, M. K. Bhaskar, C. T. Nguyen, J. L. Pacheco, H. A. Atikian, C. Meuwly, R. M. Camacho, F. Jelezko, E. Bielejec, H. Park, M. Lončar, and M. D. Lukin, Science **354**, 847 (2016).

[19] R. Uppu, F. T. Pedersen, Y. Wang, C. T. Olesen, C. Papon, X. Zhou, L. Midolo, S. Scholz, A. D. Wieck, A. Ludwig, and P. Lodahl, Sci. Adv. **6**, eabc8268 (2020).

[20] H. Wang, J. Qin, X. Ding, M.-C. Chen, S. Chen, X. You, Y.-M. He, X. Jiang, L. You, Z. Wang, C. Schneider, J. J. Renema, S. Höfling, C.-Y. Lu, and J.-W. Pan, Phys. Rev. Lett. **123**, 250503 (2019).

[21] P. Lodahl, Quantum Sci. Technol. **3**, 013001 (2017).

[22] D. E. Chang, J. S. Douglas, A. González-Tudela, C.-L. Hung, and H. J. Kimble, Rev. Mod. Phys. **90**, 031002 (2018).

[23] M. Arcari, I. Söllner, A. Javadi, S. Lindskov Hansen, S. Mahmoodian, J. Liu, H. Thyrrestrup, E. H. Lee, J. D. Song, S. Stobbe, and P. Lodahl, Phys. Rev. Lett. **113**, 093603 (2014).

[24] A. V. Kuhlmann, J. H. Prechtel, J. Houel, A. Ludwig, D. Reuter, A. D. Wieck, and R. J. Warburton, Nat. Commun. **6**, 8204 (2015).

[25] F. T. Pedersen, Y. Wang, C. T. Olesen, S. Scholz, A. D. Wieck, A. Ludwig, M. C. Löbl, R. J. Warburton, L. Midolo, R. Uppu, and P. Lodahl, ACS Photonics **7**, 2343 (2020).

[26] D. Roy, C. M. Wilson, and O. Firstenberg, Rev. Mod. Phys. **89**, 021001 (2017).

[27] E. Sánchez-Burillo, J. García-Ripoll, L. Martín-Moreno, and D. Zueco, Faraday Discuss. **178**, 335 (2015).

[28] J.-T. Shen and S. Fan, Phys. Rev. A **76**, 062709 (2007).

[29] J.-T. Shen and S. Fan, Phys. Rev. Lett. **98**, 153003 (2007).

[30] S. Fan, S. E. Kocabaş, and J.-T. Shen, Phys. Rev. A **82**, 063821 (2010).

[31] S. Das, V. E. Elfving, F. Reiter, and A. S. Sørensen, Phys. Rev. A **97**, 043838 (2018).

[32] T. Ramos and J. J. García-Ripoll, New J. Phys. **20**, 105007 (2018).

[33] R. Trivedi, K. Fischer, S. Xu, S. Fan, and J. Vučković, Phys. Rev. B **98**, 144112 (2018).

[34] H. Zheng, D. J. Gauthier, and H. U. Baranger, Phys. Rev. A **82**, 063816 (2010).

[35] J.-F. Huang, T. Shi, C. P. Sun, and F. Nori, Phys. Rev. A **88**, 013836 (2013).

[36] C. Lee, C. Noh, N. Schetakis, and D. G. Angelakis, Phys. Rev. A **92**, 063817 (2015).

[37] S. Das, L. Zhai, M. Čepulskovskis, A. Javadi, S. Mahmoodian, P. Lodahl, and A. S. Sørensen, arXiv:1912.08303.

[38] K. G. L. Pedersen and M. Pletyukhov, Phys. Rev. A **96**, 023815 (2017).

[39] J. Lang, D. E. Chang, and F. Piazza, Phys. Rev. A **102**, 033720 (2020).

[40] T. Shi, D. E. Chang, and J. I. Cirac, Phys. Rev. A **92**, 053834 (2015).

[41] T. Shi, Y. Chang, and J. J. García-Ripoll, Phys. Rev. Lett. **120**, 153602 (2018).

[42] S. Bera, A. Nazir, A. W. Chin, H. U. Baranger, and S. Florens, Phys. Rev. B **90**, 075110 (2014).

[43] D. Witthaut, M. D. Lukin, and A. S. Sørensen, Europhys. Lett. **97**, 50007 (2012).

[44] T. C. Ralph, I. Söllner, S. Mahmoodian, A. G. White, and P. Lodahl, Phys. Rev. Lett. **114**, 173603 (2015).

[45] O. Firstenberg, T. Peyronel, Q.-Y. Liang, A. V. Gorshkov, M. D. Lukin, and V. Vuletić, Nature (London) **502**, 71 (2013).

[46] S. Mahmoodian, G. Calajó, D. E. Chang, K. Hammerer, and A. S. Sørensen, Phys. Rev. X **10**, 031011 (2020).

[47] T. Ramos and J. J. García-Ripoll, Phys. Rev. Lett. **119**, 153601 (2017).

[48] P. Türschmann, H. Le Jeannic, S. F. Simonsen, H. R. Haakh, S. Götzinger, V. Sandoghdar, P. Lodahl, and N. Rotenberg, Nanophotonics **8**, 1641 (2019).

[49] P. Lodahl, S. Mahmoodian, S. Stobbe, A. Rauschenbeutel, P. Schneeweiss, J. Volz, H. Pichler, and P. Zoller, Nature (London) **541**, 473 (2017).

[50] T. Ramos, H. Pichler, A. J. Daley, and P. Zoller, Phys. Rev. Lett. **113**, 237203 (2014).

[51] See Supplemental Material at http://link.aps.org/supplemental/10.1103/PhysRevLett.126.023603 for (i) the modeling of the QD-waveguide system and measurements, including all experimental imperfections, and for (ii) the derivation of the two-photon reconstruction formulas, which additionally includes Refs. [52–54].

[52] C. W. Gardiner and P. Zoller, *Quantum Noise* (Springer-Verlag, Berlin, Heidelberg, 2004).

[53] A. Auffèves-Garnier, C. Simon, J.-M. Gérard, and J.-P. Poizat, Phys. Rev. A **75**, 053823 (2007).

[54] K. J. Blow, R. Loudon, S. J. D. Phoenix, and T. J. Shepherd, Phys. Rev. A **42**, 4102 (1990).

[55] T. Ramos (to be published).

[56] G. Kiršanskė, H. Thyrrestrup, R. S. Daveau, C. L. Dreeßen, T. Pregnolato, L. Midolo, P. Tighineanu, A. Javadi, S. Stobbe, R. Schott, A. Ludwig, A. D. Wieck, S. I. Park, J. D. Song, A. V. Kuhlmann, I. Söllner, M. C. Löbl, R. J. Warburton, and P. Lodahl, Phys. Rev. B **96**, 165306 (2017).

[57] X. Zhou, I. Kulkova, T. Lund-Hansen, S. Lindskov Hansen, P. Lodahl, and L. Midolo, Appl. Phys. Lett. **113**, 251103 (2018).

[58] M. Meissner, Acta Phys. Pol. A **121**, A-164 (2012).

[59] J. Hansom, C. H. H. Schulte, C. Matthiesen, M. J. Stanley, and M. Atatüre, Appl. Phys. Lett. **105**, 172107 (2014).